Cell Calcium 134 (2026) 103119

Contents lists available at ScienceDirect

Cell Calcium

journal homepage: www.elsevier.com/locate/ceca

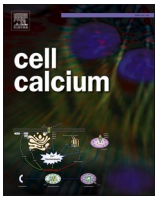

BDNF prevents amyloid-β-induced exacerbation of mGluR5-driven Ca^{2+} transients in astrocytes through TrkB-Tc activation

Pedro Avelar [a,1], Tatiana P. Morais [a,e,f,1,3], Haissa de Castro-Abrantes [a,g,4], Adam Armada-Moreira [a,d,h,5], Joana Gonçalves-Ribeiro [a,b,c], Cláudia A. Valente [a,b,c], Ana Maria Sebastião [a,b,c], Maria José Diógenes [a,b,c,2,*], Sandra H. Vaz [a,b,c,2,*]

[a] Faculdade de Medicina, Universidade de Lisboa, Portugal
[b] Centro Cardiovascular da Universidade de Lisboa, CCUL (CCUL@RISE), Faculdade de Medicina, Universidade de Lisboa, Portugal
[c] Gulbenkian Institute for Molecular Medicine (GIMM), Lisbon, Portugal
[d] Interdisciplinary Nanoscience Center (iNANO), Aarhus University, Aarhus, Denmark
[e] Life and Health Sciences Research Institute (ICVS), School of Medicine, University of Minho, Braga, Portugal
[f] ICVS/3B's-PT Government Associate Laboratory, Braga, Portugal
[g] Laboratory of Behavioural Neuroscience, Brain Mind Institute, École Polytechnique Fédérale de Lausanne, Lausanne, Switzerland
[h] Department of Biomedical, Metabolic and Neural Sciences, University of Modena and Reggio Emilia, Modena, Italy

ARTICLE INFO

Keywords:
Astrocytes
Alzheimer's disease
Amyloid-β peptide (Aβ)
Brain-derived neurotrophic factor (BDNF)
Calcium (Ca^{2+}) signaling
Metabotropic glutamate receptor type 5 (mGluR5)
TrkB-Tc receptor

ABSTRACT

Brain-derived neurotrophic factor (BDNF) is a neurotrophin that, through the activation of its full length receptor, TrkB-FL, plays a pivotal role in neuroprotection, namely against neuronal toxicity mediated by amyloid-β peptide (Aβ). In astrocytes, the increase of calcium (Ca^{2+}) signaling due the increase of metabotropic glutamate receptor type 5 (mGluR5) levels, induced by Aβ, has been considered deleterious for astrocytic function. In adition BDNF also increases intracellular calcium concentration ($[Ca^{2+}]_i$), in astrocytes, via activation of the truncated TrkB receptor isoform, TrkB-Tc. While the role of BDNF, in neurons, is well established, in terms of neuroprotection, its role in astrocytes, particularly in Aβ-induced toxicity conditions, remains less clear. Thus, this study aimed to evaluate the interplay between BDNF and Aβ in the modulation of $[Ca^{2+}]_i$ signaling in primary cultures of cortical astrocytes.

Ca^{2+} transients were induced by the activation of mGluR5 through the application of its agonist DHPG. In astrocytes pre-exposed to $Aβ_{25–35}$ (10 μM, for 48–72 h), the Ca^{2+} transient amplitude was significantly increased compared to the control. A similar increase was observed in astrocytes incubated for 48 h with BDNF (20 ng/mL), or when astrocytes were simultaneously exposed to BDNF and Aβ. The effect of BDNF was mediated by TrkB-Tc since it was prevented by a cocktail of the three siRNAs against TrkB-Tc expression. mGluR5 levels were significantly increased in astrocytes pre-exposed to Aβ, while exposure to BDNF did not affect mGluR5 levels. Importantly, while the presence of Aβ did affect TrkB-Tc receptor levels in astrocytes, the presence of BDNF prevented the increase in mGluR5 levels caused by Aβ thus precluding a further exacerbation of Ca^{2+} transients caused by Aβ.

1. Introduction

Alzheimer's disease (AD) is a common and incurable neurodegenerative disease affecting the Central Nervous System (CNS) firstly manifested by the loss of episodic memory and later by the loss of executive functions like language, attention, and reasoning [1]. One of

* Corresponding authors.
E-mail addresses: diogenes@medicina.ulisboa.pt (M.J. Diógenes), svaz@medicina.ulisboa.pt (S.H. Vaz).
[1] These authors contributed equally: Pedro Avelar and Tatiana P. Morais
[2] These authors contributed equally: Maria José Diógenes and Sandra H. Vaz
[3] Current address: Life and Health Sciences Research Institute (ICVS), School of Medicine, University of Minho, Campus Gualtar, Braga, Portugal
[4] Current address: Laboratory of Behavioural Neuroscience, Brain Mind Institute, École Polytechnique Fédérale de Lausanne, Lausanne, Switzerland
[5] Current address: Department of Biomedical, Metabolic and Neural Sciences, University of Modena and Reggio Emilia, Modena, Italy

https://doi.org/10.1016/j.ceca.2026.103119
Received 21 July 2025; Received in revised form 22 December 2025; Accepted 9 January 2026
Available online 16 January 2026

the hallmarks of AD pathogenesis is the formation of toxic amyloid-β (Aβ) species and their accumulation in the brain [2]. This mechanism leads to increased glutamate levels and overactivation of NMDA receptors that culminate in excitotoxicity and neurodegeneration detected in the brain of AD patients [3,4].

Astrocytes are the principal homeostatic cells of the CNS, having important roles in maintaining normal brain physiology. Accordingly, astrocytes are important for the formation of growth tracts during development, the preservation of the blood-brain barrier integrity, in immune responses acting as macrophages, the production of neurotrophic factors, and the support of synaptic function and plasticity [5–9]. In AD, astrocytic functions are dysregulated [10,11]. Although the mechanisms underlying the loss of astrocytic function in AD are not yet fully understood, Ca^{2+} signaling dysfunction has been considered as a key event in this process [10] since Aβ disrupts gliotransmission by exarcerbating Ca^{2+}signaling in astrocytes [12]. Indeed, astrocytes isolated from the brain of AD animal models, as well as astrocytes in culture pre-treated with Aβ have been shown to display enhanced Ca^{2+}transients [13–17]. This has been associated with the Aβ-induced increase in levels of metabotropic glutamate receptor type 5 (mGluR5) and inositol 1,4,5-trisphosphate receptor ($InsP_3R$) [16,18].

The brain-derived neurotrophic factor (BDNF), through the activation of its cognate receptor TrkB-FL in neurons, plays a crucial role in neuronal survival, differentiation, and plasticity. In addition, BDNF can activate the truncated forms of TrkB receptors: TrkB-Tc and $p75^{NTR}$ receptors in both neurons and astrocytes [19–21]. It is widely known that BDNF signaling is severely disrupted in AD patients. Indeed, there are decreased levels of BDNF and TrkB-FL receptors and increased levels of TrkB-Tc and $p75^{NTR}$ receptors in the brain of AD patients [22–28]. In our previous work, we found, in neuronal cell cultures, that Aβ, through extrasynaptic NMDA receptors activation, promotes the increase of intracellular Ca^{2+} levels, leading to the overactivation of calpains, which then promote TrkB-FL cleavage [25–27,29,30]. This process leads to the decrease of TrkB-FL levels and the generation of two distinct fragments: a membrane-bound truncated receptor (TrkB-T') and an intracellular fragment (TrkB-ICD) [25,29]. In astrocytes, the main BDNF receptor is a truncated form, the TrkB-Tc, which is not generated by cleavage but rather by alternative splicing [31].

The overall knowledge on the role of BDNF in neuropathological conditions and its dysregulation in AD is now considerably robust and detailed in neurons [25,27]. However, the information about BDNF signaling alterations in glial cells is scarce. Therefore, in the present work, we aimed at investigating the reciprocal influence of BDNF and Aβ upon Ca^{2+} signaling in astrocytes. We found that the presence of Aβ did not alter the levels of TrkB-Tc and that BDNF, through TrkB-Tc, increases astrocytic Ca^{2+} transient amplitude induced by mGluR5 activation, being devoid of influence upon mGluR levels. Notably, BDNF prevented the upregulation of mGluR levels induced by Aβ, mitigating the subsequent enhancement of Ca^{2+} signaling caused by Aβ.

2. Methods and materials

2.1. Primary astrocytic cultures

Primary cultures of cortical astrocytes were prepared from pups (postnatal day 0–2) of Sprague Dawley rats (Charles River Laboratories, Barcelona, Spain), as routinely performed in our lab [32,33]. Briefly, pups were sacrificed by decapitation and the heads were dissected under sterile conditions. The cerebellum, white matter, and meninges were carefully removed in cold phosphate-buffered saline solution (PBS) (in mM: 140 NaCl, 2.7 KCl, 1.5 KH_2PO_4, and 8.1 $NaHPO_4$; pH adjusted to 7.4). The cortex was mechanically dissociated with a 10 mL pipette in 4.5 g/L glucose Dulbecco's Modified Eagle's Medium (DMEM) (Gibco/Invirogen®, Paisley, UK), filtered through meshes of 230 μm and centrifuged at 1 200 rpm for 10 min at 20 °C. The pellet was resuspended in 4.5 g/L glucose DMEM supplemented medium, filtered through a 70 μm cell strainer (BD Falcon®, Erembodegem, Belgium), and centrifuged at 1 200 rpm for 10 min at 20 °C.

Astrocytes were seeded at a density of 38×10^4 cells/mL in T-75 (75 cm^2) culture flasks for intracellular Ca^{2+} measurements or in 12-well plates for western blot experiments.

Astrocytes were maintained for up to 11–13 days in culture (DIC). Culture medium (5 g/L glucose DMEM medium containing 10 % fetal bovine serum (FBS, Gibco, Paisley, UK) with 0.01 % antibiotic/antimycotic (Sigma, Steinheim, Germany)) was changed on the third, sixth, and seventh day after seeding.

Microglia contamination was minimized by following a standard shaking procedure [34]. Once cultures reached confluence (DIC 7), loosely attached microglia on the astrocyte monolayer were removed by horizontal shaking at 300 rpm for 3–5 h at 37 °C in a 5 % CO_2 atmosphere. The adherent astrocytes were enzymatically dispersed (0.025 % trypsin-EDTA, Sigma, Stenheim, Germany) under agitation for 2 min at 37 °C and the reaction was stopped by adding an excess of 4.5 g/L glucose DMEM supplemented medium. To validate the astrocytic culture immunocytochemistry assays were made (**Supp. Fig. 1**). Astrocytes to be used in Ca^{2+} imaging experiments were plated (7×10^4 cells/mL) over γ-irradiated glass-bottom microwell dishes with a glass thickness of 0.16–0.19 mm and a glass diameter of 14 mm (MatTek® Corporation, Ashland, MA, USA), previously coated with poly(D-lysine) (10 μg/mL) for 1 hour and washed with sterile water (3 times), to improve cell adhesion.

Astrocytes plated in γ-irradiated glass bottom microwell dishes and in 12-well plates were pharmacologically treated at DIC 10 and used for Ca^{2+} imaging experiments and western blot technique respectively, from DIC 11 to DIC 13.

2.2. Ca^{2+} imaging

Ca^{2+} imaging was performed as previously described [35]. All the experiments were performed at room temperature of 22 °C (RT), using the fluorescent Ca^{2+} dye Fura-2AM (Calbiochem, Darmstadt, Germany).

Before each experiment, cells seeded in a γ-irradiated glass bottom microwell dish were gently washed with HEPES buffer (3 times) (in mM: 125 NaCl, 3 KCl, 1.25 NaH_2PO_4, 10 Glucose, 10 HEPES, 2 $CaCl_2$, 2 $MgSO_4$; pH ~ 7.38), to remove any traces of previous medium (DMEM). Afterward, cells were incubated with 5 μM Fura-2AM in HEPES buffer at 22 °C for 45 min. Again, cells were gently washed with HEPES buffer to remove any traces of extracellular Fura-2AM deposits.

The γ-irradiated glass bottom microwell dish containing the plated cells was placed on the stage of an inverted epifluorescence microscope (Axiovert 135TV, Zeiss®, Oberkochen, Germany) with a 40x oil objective and equipped with a xenon lamp and band-pass filters of 340 and 380 nm wavelengths.

Using a rotating pump system (Mini PIL3, GILSON®, Middleton, USA), the perfusion medium (HEPES buffer) was continuously loaded into the cell plate, at a rate of approximately 1.5 mL/min. At the beginning of each experiment, cells were placed at rest in the microscope platform for about 5 min for temperature stabilization.

Ca^{2+} transients were induced by the focal application of the mGluR5 receptor agonist (*S*)-3,5-Dihydroxyphenylglycine (DHPG), through a drug-filled micropipette placed under visual guidance over a single astroglial cell. The DHPG focal application was achieved by focal pressure (10 psi for 2 s) through a pressurized system (Toohey Company®, New Jersey, USA), at 5 min (300 s) time intervals. The DHPG (10 μM) focal stimulation was repeated 5 times for each cell and a last stimuli (6th) was made with 100 μM DHPG. The final DHPG (100 μM) stimulus was performed to achieve a maximal transient amplitude mediated by mGluR5 receptor activation. The concentration of mGluR5 receptor agonist referred to in this work were those in the micropipette filling solution. Pressure application of external physiological solution did not cause any measurable change in intracellular Ca^{2+} concentration (data not shown).

Image pairs were obtained every 250 ms by exciting Fura-2AM-loaded astrocytes sequentially at 340 nm and 380 nm. Excitation wavelengths were changed through a high-speed wavelength switcher, Lambda DG-4 (Sutter Instrument, Novato, CA, USA), and the emission wavelength was set to 510 nm. Image data were recorded with a cooled CCD camera (Photometrics CoolSNAP fx, Tucson, USA) and processed and analyzed using the software MetaFluor (Universal Imaging, West Chester, PA, USA), which automatically subtracts background fluorescence and autofluorescence. Regions of interest were defined manually over the cell profile. The software also calculated and reported, in real-time, the fluorescence ratio F340/F380, and this parameter was used to monitor $[Ca^{2+}]_i$ changes [36,37]. The kinetics of Ca^{2+} transients was analysed using the script described by Lopes et al. [38].

2.3. Western blot

Between DIC 11 and DIC 13, cells were washed twice with cold PBS (in mM: 137 NaCl, 2.1 KCl, 1.8 KH_2PO_4, 10 NaH_2PO_4) and then lysed with 1 % NP-40 lysis buffer containing (in mM): 150 NaCl, 50 Tris–HCl (pH 7.5), ethylenediaminetetraacetic acid (EDTA), and EDTA-free protease inhibitor cocktail (Roche®, Basel, Switzerland). Cell lysates were clarified by centrifugation (13 000 rpm, 10 min, at 4 °C), and the amount of protein in the supernatant was determined by Bio-Rad DC reagent.

Each sample (40 μg of total protein) was separated in 10 % sodium dodecyl sulfate-polyacrylamide gel electrophoresis (SDS–PAGE) and transferred onto polyvinylidene difluoride (PVDF) membranes (GE Healthcare). Membranes were stained with Ponceau S solution to check for protein transference efficacy. After blocking with a 5 % nonfat dry milk solution in TBS-Tween (20 mM Tris base, 137 mM NaCl, and 0.1 % Tween-20), membranes were incubated with the primary (overnight at 4 °C) and secondary antibodies (1 h at room temperature). Finally, immunoreactivity was visualized using ECL chemiluminescence detection system (Amersham-ECL Western Blotting Detection Reagents, GE Healthcare), and band intensities were quantified by digital densitometry (ImageJ 1.45 software [39]). The intensity of β-actin or Ponceau S bands were used as the loading control.

2.4. Transfection with siRNAs

For transient silencing of TrkB-Tc receptor, three different rat double-stranded TrkB-T small interfering (si) RNAs (30 nM) (Ambion, Austin, TX, USA), designed with the Integrated DNA Technologies (Coralville, IA), were used and validated [40]. Additionally, a cocktail of the three siRNAs (RNAi 1/2/3), a negative control with scrambled siRNA, and a mock control performed in the absence of siRNA were tested. To transfect the astrocytes, the reverse transfection method with siPORT Amine (Ambion) was used according to the manufacturer's guidelines. Briefly, DIC 9 astrocytes were trypsinized, resuspended in DMEM at a density of 8×10^4 cells/mL, and transfected as they adhere to the plate. After 18 h of incubation with transfection complexes, cell medium was replaced with fresh DMEM. All experiments were performed 72 h after transfection.

2.5. Immunocytochemistry assay

For immunocytochemistry, cells at DIC 21–23 were washed twice with PBS (pH 7.4) for 5 min and fixed with 4 % paraformaldehyde (PFA) for 15 min at room temperature (RT). Residual PFA was quenched by incubation with freshly prepared 0.1 M glycine in PBS for 10 min at RT. Cells were then permeabilized with 0.5 % Triton X-100 in PBS for 10 min at RT and washed twice with PBS. To reduce non-specific binding, cells were incubated in blocking solution (PBS containing 10 % FBS) for 1 h at RT. Glass coverslips were removed from the 24-well plates and incubated (cells facing down) overnight at 4 °C in 20 μL drops of blocking solution containing mouse anti-GFAP primary antibody (1:400). The following day, coverslips were returned to the 24-well plates (cells facing up) and washed three times for 5 min with PBS containing 0.2 % Tween-80 (PBS-Tw). Coverslips were then incubated for 1 h at RT in 20 μL drops of goat anti-mouse IgG conjugated to Alexa Fluor 568 (1:1000) diluted in blocking solution, followed by three 5-min washes with PBS-Tw. Nuclei were stained with DAPI (4′,6′-diamidino-2-phenylindole; 1:1000; Invitrogen, USA) for 5 min at RT in the dark, and coverslips were washed three times with PBS-Tw for 10 min. After drying, coverslips were mounted (cells facing down) onto glass slides using 4 μL of Mowiol mounting medium (Sigma, Steinheim, Germany) and allowed to cure for 24 h at RT. Slides were then stored at 4 °C.

2.6. Reagents and drug treatment

Amyloid-β and control peptides were purchased from Bachem and prepared in sterile deionized water. Unless otherwise specified, $A\beta_{25–35}$ and $A\beta_{35–25}$ were used at 10 μM (100 × stock solution). Stock solutions of BDNF (kindly supplied by Regeneron Pharmaceuticals (Tarrytown, NY)) were prepared in PBS at a final concentration of 1 mg/mL. BDNF was used in a final concentration of 20 ng/mL, as previously described by Jerónimo-Santos and colleagues [29].

Astrocytes were plated on γ-irradiated glass-bottom microwell dishes and 12-well plates, and pharmacologically treated on DIC 10 with Aβ25–35, Aβ35–25, or BDNF. From DIC 11 to DIC 13, cells were used for intracellular Ca^{2+} imaging (microwell dishes) and western blot analysis (12-well plates), respectively.

(*S*)-3,5-Dihydroxyphenylglycine (DHPG) was acquired from Tocris (Bristol, UK) and was used at the final concentrations of 10 μM and/or 100 μM.

Antibodies were purchased from the following sources: the mGluR5 rabbit polyclonal antibody (1:4 000), raised against the extracellular domain of human mGluR5, from Millipore, the TrkB mouse polyclonal antibody (1:1 500), raised against the extracellular domain of human TrkB (aa. 156–322), from BD Bioscience, the αII-spectrin (c-3) mouse monoclonal antibody (1:500), raised against human spectrin (aa-2 368–2 472), from Santa Cruz, Inc, the anti-GFAP mouse monoclonal from Sigma-Aldrich, and the β-actin rabbit polyclonal antibody (1:5 000) from Abcam. The IgG-horseradish peroxidase-conjugated secondary antibodies used were goat anti-mouse (1:10 000) and goat anti-rabbit (1:10 000) (Santa Cruz).

2.7. Statistical analysis

Values are presented as the mean ± standard error of the mean (SEM). For the Ca^{2+} imaging experiments herein reported, *n* represents the number of individual responsive cells. In each experiment, a field with *n* responsive cells was selected and their response (wave amplitude) to the stimulus (pressure applied mGluR5 receptor agonist) was quantified for each of the drug pre-treatments conditions. The transient amplitude was calculated as the average of five individual responses to DHPG (10 μM) stimulation, determined by subtracting the baseline level (measured over 20 acquisition cycles prior to stimulation) from the maximum peak value. For western blot, *n* represents the number of independent experiments, i.e., independently prepared primary cultures of astrocytes prepared from P0-P2 Sprague Dawley pups. All statistical analyses were performed with GraphPad Prism software. For multiple comparisons made between three or more conditions, a simple analysis of variance (one-way ANOVA) was used, followed by a *Tukey* test. Values with a *p-value* of < 0.05 were considered statistically significant ($^*P < 0.05$; $^{**}P < 0.01$; $^{***}P < 0.001$; $^{****}P < 0.001$).

3. Results

3.1. Astrocytes incubated with Aβ have enhanced Ca^{2+} signaling and mGluR5 expression

To assess the influence of Aβ upon astrocytic Ca^{2+}signaling under our

experimental conditions, astrocytes at DIC 10 were incubated with $A\beta_{25–35}$ (10 μM) for 24 h, 48 h, and 72 h. After Aβ incubation, Ca^{2+} signals were induced by pressure-application of the mGluR agonist DHPG for 2 s, as described in the methods section. This stimulation retrieves a strong and fast Ca^{2+} peak that returned to basal levels approximately 10 s after the stimulus. Since the Ca^{2+} signals detected with Fura-2 predominantly reflect cytosolic Ca^{2+} dynamics [41], the fast and transient responses observed following DHPG application are characteristic of IP_3-dependent Ca^{2+} release from endoplasmic reticulum stores [42] and are inconsistent with mitochondrial Ca^{2+} signals, which are typically slower and more sustained [43]. In astrocytes treated with $A\beta_{25–35}$ for 48 h or 72 h, the ratio F340/380 for the Ca^{2+} transients was significantly increased as compared to astrocytes incubated under control condition (Fig. 1**A-C**; CTR: 8.70 ± 0.35, $n = 55$ cells, from 7 independent cultures; $A\beta_{25–35}$ 48h: 10.4 ± 0.41, $n = 24$ cells and $A\beta_{25–35}$ 72h: 10.4 ± 0.49, $n = 31$ cells, from 7 independent cultures, one-way ANOVA followed by Bonferroni's post hoc test, $P < 0.0001$). Importantly, astrocytes pre-treated with the scrambled Aβ ($A\beta_{35–25}$) for 48 h did not present significant differences in Ca^{2+} transient amplitude when compared with astrocytes in a vehicle situation (**Supp. Fig. 2).**

Interestingly, the basal Ca^{2+} levels in astrocytes pre-exposed to $A\beta_{25–35}$ for 48 h or 72 h were appreciably different from control astrocytes even before starting the first stimulation with DHPG (Fig. 1**D**, $CTR_{basal\ Ca2+level}$: 1.99 ± 0.015, $n = 55$ cells, from 7 independent cultures; $A\beta_{25–35(24\ h)\text{-}basal\ Ca2+level}$: 1.97 ± 0.007, $n = 47$ cells, from 7 independent cultures; $A\beta_{25–35(48\ h)\text{-}basal\ Ca2+level}$: 3.14 ± 0.015, $n = 24$ cells from 7 independent cultures; $A\beta_{25–35(72\ h)\text{-}basal\ Ca2+level}$: 2.87 ± 0.013, $n = 31$ cells, from 7 independent cultures; two-way ANOVA followed by Tukey's post hoc test, $P < 0.0001$). Moreover, the basal Ca^{2+}levels progressively increased along with stimulation with DHPG for all tested conditions (Fig. 1**D**), with the change between the F340/380 values before the last and the first stimulation (Δ[5th stimulation-1st stimulation]) being significantly different in astrocytes incubated with $A\beta_{25–35}$ for 24 h, 48 h or 72 h compared to control astrocytes (Fig. 1**E**; CTR: 0.48 ± 0.03, $n = 55$ cells, from 7 independent cultures; $A\beta_{25–35(24\ h)}$: 0.83 ± 0.09, $n = 47$ cells, from 7 independent cultures, $A\beta_{25–35(48\ h)}$: 1.47 ± 0.08, $n = 24$ cells, from 7 independent cultures, and $A\beta_{25–35(72\ h)}$: 1.59 ± 0.04, $n = 31$ cells, from 7 independent cultures, one-way ANOVA followed by Bonferroni's *post hoc* test, $P < 0.0001$).

Analysis of the kinetics of the Ca^{2+} transients revealed a significant decrease in rise time only in astrocytes pre-exposed to $A\beta_{25–35}$ for 48 h or 72 h (Fig. 1**H** and **I**; CTR: 8.8 ± 1.2 s, from 5 independent cultures; $A\beta_{25–35(24\ h)}$: 8.4 ± 0.87 s, from 5 independent cultures; $A\beta_{25–35(48\ h)}$: 4.4 ± 0.24 s, from 5 independent cultures; $A\beta_{25–35(72\ h)}$: 5.4 ± 0.50 s, from 5 independent cultures; one-way ANOVA followed by Tukey's post hoc test, $P < 0.05$). No significant changes were observed in the decay time of the Ca^{22+} transients (Fig. 1**H** and **J**; CTR: 24.0 ± 2.0 s, from 5 independent cultures; $A\beta_{25–35(2\ h)}$: 24.0 ± 2.0 s, from 5 independent cultures; $A\beta_{25–35(48\ h)}$: 22.0 ± 2.6 s, from 5 independent cultures; $A\beta_{25–35(72\ h)}$: 24.4 ± 1.7 s, from 5 independent cultures; one-way ANOVA followed by Tukey's post hoc test).

In accordance with previous reports [15,16], in astrocytes pre-treated with $A\beta_{25–35}$ for 48 h and 72 h, mGluR5 levels were significantly increased (Fig. 1**F,G**, CTR: 1.00, $n = 7$; $A\beta_{25–35}$ 48h: 1.32 ± 0.0670, $n = 7$; $A\beta_{25–35}$ 72h: 1.35 ± 0.130, $n = 5$; one-way ANOVA followed by Bonferroni's *post hoc* test, $P < 0.05$ when compared to astrocytes pre-treated with vehicle), with said increase in the order of 32–35 %. As a control, the levels of mGluR5 were evaluated in astrocytes that had been in the presence of the scrambled $A\beta_{35–25}$ (10 μM). The presence of scrambled Aβ for the duration as that used to expose astrocytes to $A\beta_{25–35}$ did not alter the levels of mGluR5 receptors compared with those in astrocytes incubated under control conditions (**Supp. Fig. 3**).

3.2. Effect of BDNF on the Ca^{2+} signaling and its interference with Aβ

Astrocytes at DIC 10 were treated with BDNF (20 ng/mL) for 48 h in the presence or absence of $A\beta_{25–35}$ (10 μM) and calcium transients were elicited by pressure application of mGluR agonist DHPG (Fig. 2**A**). Similar to what had been observed in astrocytes exposed to $A\beta_{25–35}$, the ratio F340/380 was significantly increased, by approximately 50 %, in astrocytes exposed to BDNF alone compared to astrocytes pre-exposed to the vehicle (Fig. 2**B**; CTR: 8.57 ± 0.370, $n = 56$ cells; BDNF: 12.8 ± 0.650, $n = 14$ cells, from 4 independent cultures, one-way ANOVA followed by Bonferroni's post hoc test, $P < 0.0001$). Interestingly, the simultaneous incubation with $A\beta_{25–35}$ and BDNF did not lead to a further increase in Ca^{2+} transient amplitude as compared with each drug alone. While the amplitude of Ca^{2+} transients was significantly increased by nearly 30 % in astrocytes exposed to $A\beta_{25–35}$ and BDNF when compared with astrocytes pre-treated with vehicle (Fig. 2**B**; CTR: 8.57 ± 0.370, $n = 56$ cells; $A\beta_{25–35}$ + BDNF: 11.1 ± 0.674, $n = 21$ cells, from 4 independent cultures, one-way ANOVA followed by Bonferroni's post hoc test, $P = 0.0014$), no statistically significant differences were found in relation to the values attained in astrocytes incubated with each drug alone.

Regarding basal Ca^{2+}levels, astrocytes pre-exposed to all drugs alone or in combination (except to $A\beta_{35–25}$) presented significant increases when compared to control astrocytes, even before starting the first stimulation with DHPG (Fig. 2**C**, $CTR_{basal\ Ca2+level}$: 1.99 ± 0.015, $n = 34$ cells, from 4 independent cultures; $A\beta_{25–35(48\ h)\text{-}basal\ Ca2+level}$: 3.09 ± 0.049, $n = 24$ cells, from 4 independent cultures; $BDNF_{(48\ h)\text{-}basal\ Ca2+level}$: 3.14 ± 0.013, $n = 18$ cells from 4 independent cultures; BDNF+$A\beta_{25–35(48\ h)\text{-}basal\ Ca2+level}$: 3.09 ± 0.021, $n = 29$ cells from 4 independent cultures; two-way ANOVA followed by Tukey's post hoc test, $P < 0.001$). The progressive increase in basal Ca^{2+} levels was observed throughout the DHPG stimulations, with the change between the F340/380 values before the last and the first stimulation (Δ[5th stimulation-1st stimulation]) being significantly different in control astrocytes and astrocytes incubated with BDNF, $A\beta_{25–35}$ or BDNF+$A\beta_{25–35}$ (Fig. 2**C**).

Analysis of the kinetics of the Ca^{2+} transients revealed a significant decrease in rise time only in astrocytes pre-exposed to $A\beta_{25–35}$ and BDNF (Fig. 2**D and E**; CTR: 8.8 ± 1.2 s, from 5 independent cultures; BDNF + $A\beta_{25–35(24\ h)}$: 4.4 ± 0.68 s, from 5 independent cultures; BDNF: 6.2 ± 0.37 s, from 5 independent cultures; one-way ANOVA followed by Tukey's post hoc test, $P < 0.05$). No significant changes were observed in the decay time of the Ca^{2+} transients (Fig. 2**D and F**; CTR: 24.0 ± 2.0 s, from 5 independent cultures; BDNF + $A\beta_{25–35(24\ h)}$: 22.8 ± 2.33 s, from 5 independent cultures; BDNF: 22.6 ± 2.46 s, from 5 independent cultures; one-way ANOVA followed by Tukey's post hoc test).

3.3. Impact of BDNF on mGluR5 levels in astrocytes

We then investigated whether the increases in Ca^{2+}transient amplitude detected in astrocytes pre-treated with BDNF for 48 h were also due to changes in mGluR5 expression levels. Data showed no significant increase in mGluR5 levels in astrocytes pre-treated with BDNF (Fig. 3**A**). Importantly, the presence of BDNF prevented the increase in mGluR5 levels caused by $A\beta_{25–35}$. (Fig. 3**A)** (CTR: 1, $n = 5$; BDNF 48h: 1.08 ± 0.13, $n = 5$; $A\beta_{25–35}$ + BDNF: 1.076 ± 0.125, $n = 5$).

3.4. BDNF increases Ca^{2+} transient amplitude through TrkB-Tc activation

TrkB-Tc is the predominant isoform of the TrkB receptor family expressed in astrocytes [44–46]. Previous reports showed that BDNF elicits Ca^{2+}signaling in cultured astrocytes by the activation of TrkB-Tc [19], so our next step was to study the impact of incubating astrocytes with BDNF and/or $A\beta_{25–35}$ on TrkB-Tc receptor levels. No significant changes in TrkB-Tc receptor levels were detected in astrocytes incubated with $A\beta_{25–35}$ (10 μM), BDNF (20 ng/mL) or $A\beta_{25–35}$ (10 μM) plus BDNF (20 ng/mL), as compared with levels in astrocytes in control conditions (Fig. 3**B**).

To evaluate if the effect of BDNF upon astrocytic Ca^{2+} transient amplitude could be attributed to the activation of TrkB-Tc, we

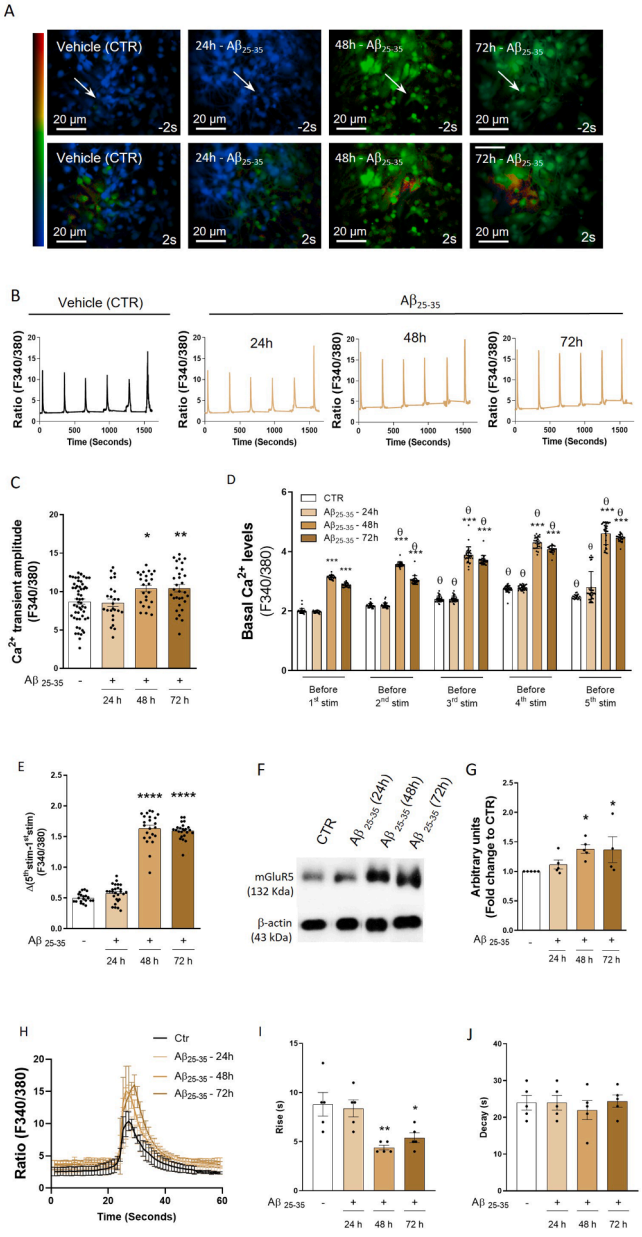

Fig. 1. Effect of Aβ upon Ca^{2+} transient amplitude and Ca^{2+}basal levels in astrocytes. A) Representative Ca^{2+} imaging 2 s before (upper panel) and after (lower panel) the focal stimulation with DHPG (10 μM), a mGluR5 agonist, which was pressure-applied for 2 s, at 5 min (300 s) time intervals (arrowhead indicates the position of the DHPG-containing pipette) in astrocytes treated with vehicle or 10 μM Aβ (24 h, 48 h or 72 h), as indicated in each panel. B) Representative graphs of single cell responses to DHPG from cultured astrocytes that have been incubated with vehicle (CTR) or $Aβ_{25–35}$ (10 μM) for 24 h, 48 h or 72 h, as indicated in each panel. Each Ca^{2+} transient was induced by DHPG at 5 min (300 s) time intervals. 5 single stimuli with DHPG (10 μM) were then followed by a last stimulus (6th) with DHPG (100 μM) to induce a maximal effect of DHPG. C) Effects of $Aβ_{25–35}$ (10 μM) at 24, 48 and 72 h (astrocytes incubated at DIC 10) upon Ca^{2+} transients induced by activation of mGluR5 in astrocytes. Mean of the 5 single stimuli with DHPG (10 μM) ± SEM of n = 25–55 cells from 7 independent cultures, *$p < 0.05$; significant differences between CTR, $Aβ_{35–25}$ (10 μM) and $Aβ_{25–35}$ (10 μM) conditions assessed by one-way ANOVA followed by Tukey correction. Only responsive cells were quantified. D) Effects of $Aβ_{25–35}$ (10 μM) at 24, 48 and 72 h upon intracellular Ca^{2+} baseline before DHPG stimulation for each performed stimulation. Mean ± SEM of n = 20–84 cells from 7 independent cultures were analyzed (***$p < 0.001$ relative to CTR within the same stimulation group; $^{\theta}p < 0.001$ relative to CTR before 1st stimulation; significant differences assessed by two-way ANOVA followed by multiple comparisons). E) Difference between the basal Ca^{2+} levels before the 5th stimulation and the 1st stimulation with DHPG (Δ(5th stim-1st stim)) for vehicle (CTR) or $Aβ_{25–35}$ (10 μM) for 24 h, 48 h or 72 h. Mean ± SEM of n = 20–84 cells from 7 independent cultures were analyzed (**$p < 0.01$; ****$p < 0.0001$; significant differences assessed by one-way ANOVA followed by Tukey correction). F) Representative image of a western blot for the detection of mGluR5 levels in control astrocytes and astrocytes incubated at DIC 10 with $Aβ_{25–35}$ (10 μM) for 24, 48, or 72 h. G) Effects of $Aβ_{25–35}$ upon mGluR5 levels in astrocytes at the different time points. Mean ± SEM of n = 5 independent cultures (*$p < 0.05$ relative to CTR assessed by one-way ANOVA followed by Tukey correction). H) Representative graphs of average Ca^{2+}single cell responses to DHPG from cultured astrocytes that have been incubated with vehicle (CTR) or $Aβ_{25–35}$ (10 μM) for 24 h, 48 h or 72 h. I) Effects of $Aβ_{25–35}$ upon rise time obtained from the kinetics of the Ca^{2+} transients induced by DHPG. J) Effects of $Aβ_{25–35}$ upon decay time obtained from the kinetics of the Ca^{2+} transients induced by DHPG. Mean ± SEM from 5 independent cultures were analyzed (*$p < 0.05$; **$p < 0.01$; significant differences assessed by one-way ANOVA followed by Tukey correction).

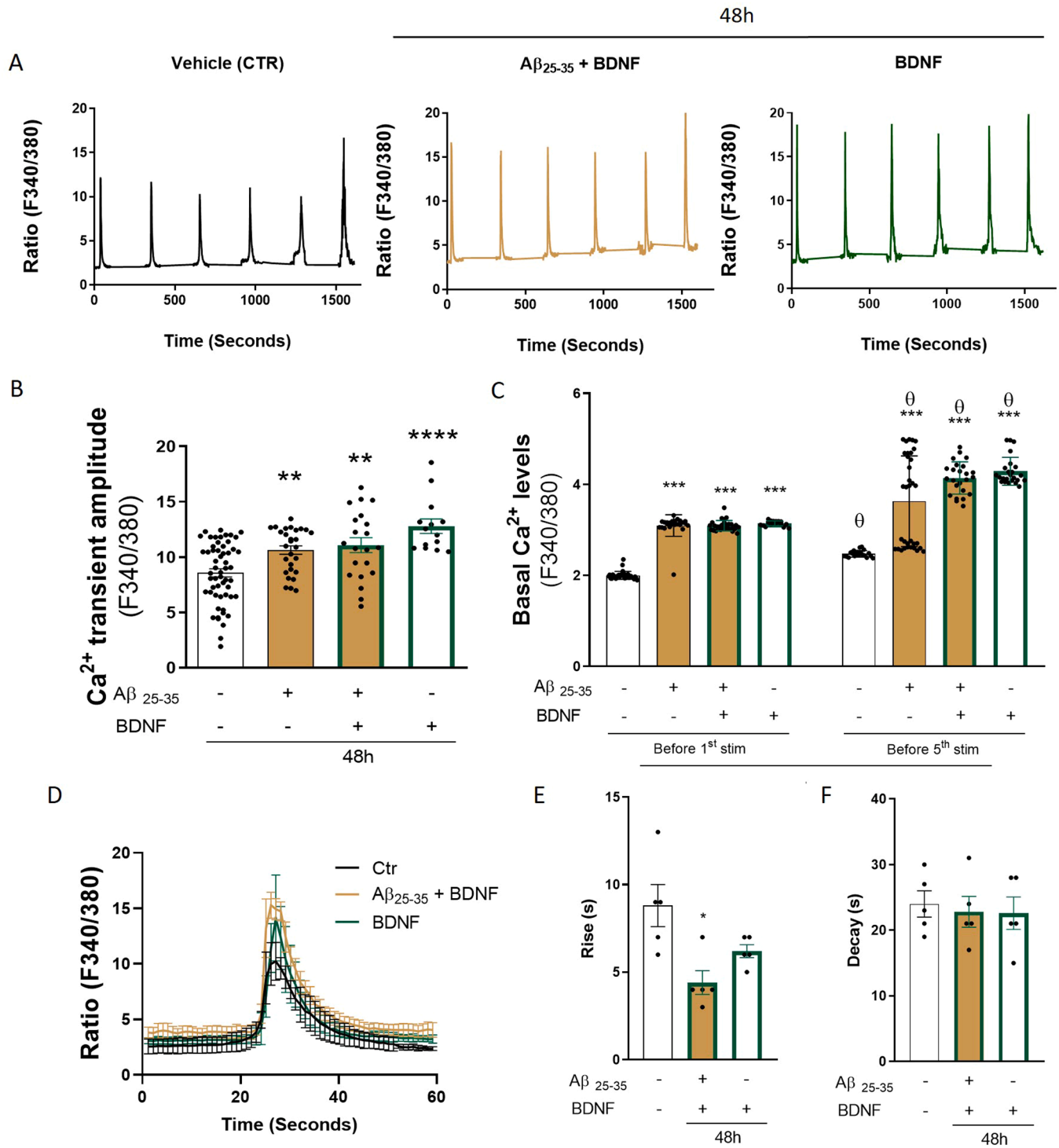

Fig. 2. Effect of BDNF upon Ca^{2+} transient amplitude and Ca^{2+} basal levels in astrocytes. A) Representative traces of a single cell responses to DHPG (10 μM) in vehicle, $A\beta_{25-35}$ (10 μM) + BDNF (20 ng/mL) 48 h and BDNF (20 ng/mL) 48 h conditions. Five stimulation were performed using DHPG (10 μM), followed by the last stimulus (6th) with DHPG (100 μM). DHPG, a mGluR5 agonist, was pressure-applied for 2 s, at 5 min (300 s) time intervals. B) Effects of $A\beta_{25-35}$ (10 μM), $A\beta_{25-35}$ (10 μM) + BDNF (20 ng/mL) and BDNF (20 ng/mL) at 48 h (astrocytes incubated at DIC 10) upon Ca^{2+} transients induced by activation of mGluR5 in astrocytes. Mean ± SEM of n = 14–56 cells from 4 independent cultures (**$p < 0.01$ and ****$p < 0.0001$; significant differences assessed by one-way ANOVA followed by Tukey correction). The results include only responsive cells. C) Effects of $A\beta_{25-35}$ (10 μM), $A\beta_{25-35}$ (10 μM) + BDNF (20 ng/mL) and BDNF (20 ng/mL) at 48 h upon intracellular Ca^{2+} baseline before DHPG stimulation for the 1st and the 5th stimulation, as indicated in the bottom of the graph. Mean ± SEM of n = 19–84 responsive cells from 4 independent cultures were analyzed (***$p < 0.001$ relative to CTR within the same stimulation group; $^{\theta}p < 0.001$ relative to CTR before 1st stimulation; significant differences assessed by two-way ANOVA followed by multiple comparisons). D) Representative graphs of average single cell Ca^{2+} responses to DHPG from cultured astrocytes that have been incubated with vehicle (Ctr), $A\beta_{25-35}$ (10 μM) + BDNF (20 ng/mL) 48 h and BDNF (20 ng/mL) 48 h conditions. E) Effects of $A\beta_{25-35}$ upon rise time obtained from the kinetics of the Ca^{2+} transients induced by DHPG. F) Effects of $A\beta_{25-35}$ upon decay time obtained from the kinetics of the Ca^{2+} transients induced by DHPG. Mean ± SEM from 5 independent cultures were analyzed (*$p < 0.05$; significant differences assessed by one-way ANOVA followed by Tukey correction).

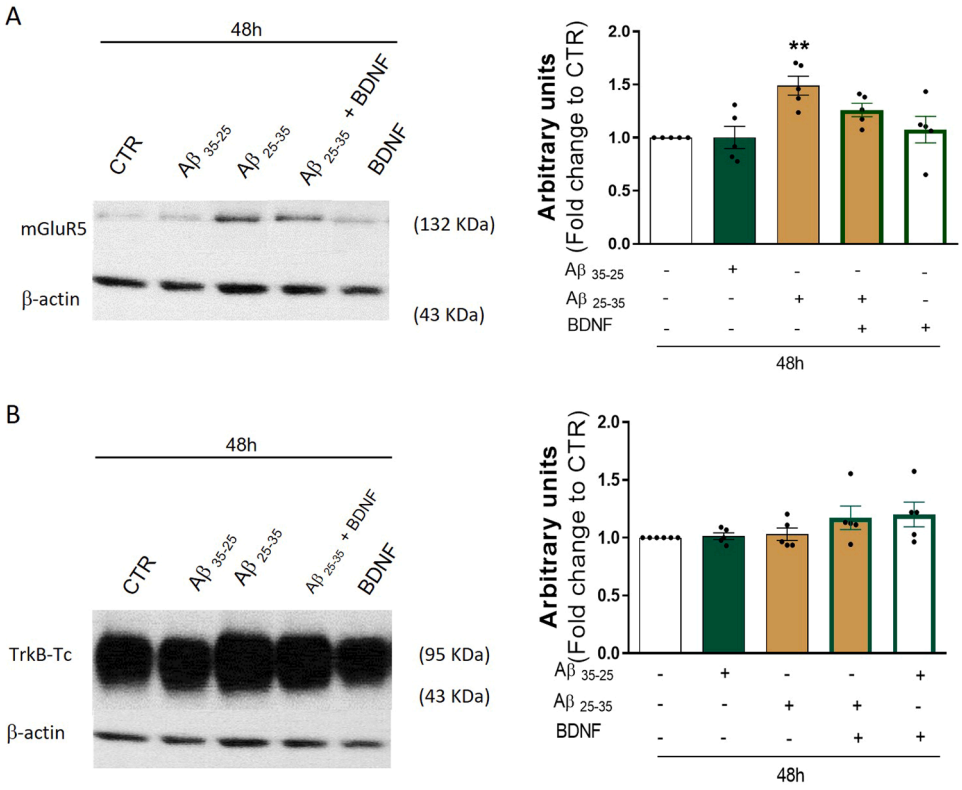

Fig. 3. Effect of Aβ and BDNF on mGluR5 and TrkB-Tc receptor levels in astrocytes. A) Left panel, representative image of a western blot for the detection of mGluR5 levels in astrocytes incubated at DIC 10 with $A\beta_{35-25}$ (10 μM), $A\beta_{25-35}$ (10 μM), $A\beta_{25-35}$ (10 μM) + BDNF (20 ng/mL), and BDNF (20 ng/mL) for 48 h. Right panel, graph plot summarizes the effects of $A\beta_{25-35}$ (10 μM), $A\beta_{25-35}$ (10 μM) + BDNF (20 ng/mL), and BDNF (20 ng/mL) at 48 h upon mGluR5 levels in astrocytes. Mean ± SEM of n = 5 independent cultures (*p < 0.05; significant differences assessed by one-way ANOVA followed by Tukey correction). B) Left panel, representative image of a western blot for the detection of TrkB-Tc levels in astrocytes incubated at DIC 10 with $A\beta_{35-25}$ (10 μM), $A\beta_{25-35}$ (10 μM), $A\beta_{25-35}$ (10 μM) + BDNF (20 ng/mL), and BDNF (20 ng/mL) for 48 h. Right panel, graph plot summarizes the effects of $A\beta_{25-35}$ (10 μM), $A\beta_{25-35}$ (10 μM) + BDNF (20 ng/mL) and BDNF (20 ng/mL) at 48 h upon TrkB-Tc levels in astrocytes. Mean ± SEM of n = 5 independent cultures (significant differences assessed by one-way ANOVA followed by Tukey correction).

performed RNA interference experiments using a cocktail of the three siRNAs (siRNA 1/2/3) to block TrkB-Tc receptor expression. Previous studies from our lab have shown that the transient transfection with a cocktail of siRNA 1/2/3 for TrkB-Tc almost completely abolished TrkB-Tc expression [40]. After a 72 h transfection of astrocytes with the cocktail siRNA 1/2/3, we observed that BDNF no longer enhanced Ca^{2+} transient amplitude (Fig. 4; $BDNF_{SiRNA1/2/3}$: 102 ± 2.81 %, calculated in relation to $CTR_{SiRNA1/2/3}$: 100 %, n = 36–87 cells, from 3 independent cultures, one-way ANOVA followed by Bonferroni's post hoc test, P = 0.9889). In contrast, the presence of scrambled siRNA, i.e. used as a negative control to assess non-specific effects of siRNA transfection, did not abolish the effect of BDNF (Fig. 4; $BDNF_{SiRNAScramble}$: 146 ± 5.11 %, calculated in relation to $CTR_{SiRNAScramble}$: 100 %, n = 74–91 cells, from 2–3 independent cultures, one-way ANOVA followed by Tukey's post hoc test, $P < 0.0001$). Similarly, mock incubation in the absence of siRNA also did not affect the action of BDNF (Fig. 4; $BDNF_{Mock}$: 123 ± 4.28 %, calculated in relation to $CTR_{SiRNAMock}$: 100 %, n = 65–68 cells, from 2–3 independent cultures, one-way ANOVA followed by Tukey's post hoc test, P = 0.0418).

3.5. *Influence of BDNF and Aβ on astrocyte viability*

To ascertain whether the changes in Ca^{2+} transients were due to alterations in astrocyte viability, αII-Spectrin levels were evaluated. αII-Spectrin is an actin binding protein. Its key role is to link the cellular plasma membrane to the actin cytoskeleton, being essential in determining the properties, including shape and deformability, of the cellular membrane. During apoptotic and necrotic cell death, calpain and caspase specific cleavage of αII-spectrin yields breakdown products (SBDPs) [47]. Therefore, the evaluation of αII-Spectron and SBDPs allows the determination of the cellular viability. Astrocytes at DIC 10 were incubated with $A\beta_{25-35}$ (10 μM) and/or BDNF (20 ng/mL) for 48 h. After Aβ and BDNF incubations, astrocyte homogenates were collected and western blot was performed, following the procedures described in the methods section. Western blot results revealed only one immunoreactive band at ~240 kDa, corresponding to αII-spectrin precursor, which was not statistically different between experimental conditions (Fig. 5). The absence of SBDPs indicates the absence of calpain or caspase activation, suggesting that cellular viability was not compromised in the conditions studied.

4. Discussion

The main findings in this work are that BDNF increases astrocytic Ca^{2+} transient amplitude induced by mGluR5 activation through a mechanism dependent on TrkB-Tc activation. Importantly, BDNF per se did not alter mGluR levels in astrocytes but prevented the increase of mGluR5 levels caused by Aβ as well as prevented a further Aβ-induced enhancement of astrocytic calcium signaling.

AD is characterized by the accumulation of intracellular hyperphosphorylated tau proteins (neurofibrillary tangles) and of extracellular plaques composed by Aβ peptides. Aβ plaques are largely composed by Aβ40 and Aβ42, but also by Aβ fragments such as $A\beta_{25-35}$ [48], which has been proposed to be the active region of the full-length Aβ peptide responsible for its neurotoxic effects [49]. The Aβ toxic effects have been mainly explored in neurons. Nevertheless, although less studied, the astrocytic functions are also compromised in AD. Indeed, Aβ has been implicated in the upregulation of α7 nicotinic acetylcholine receptors

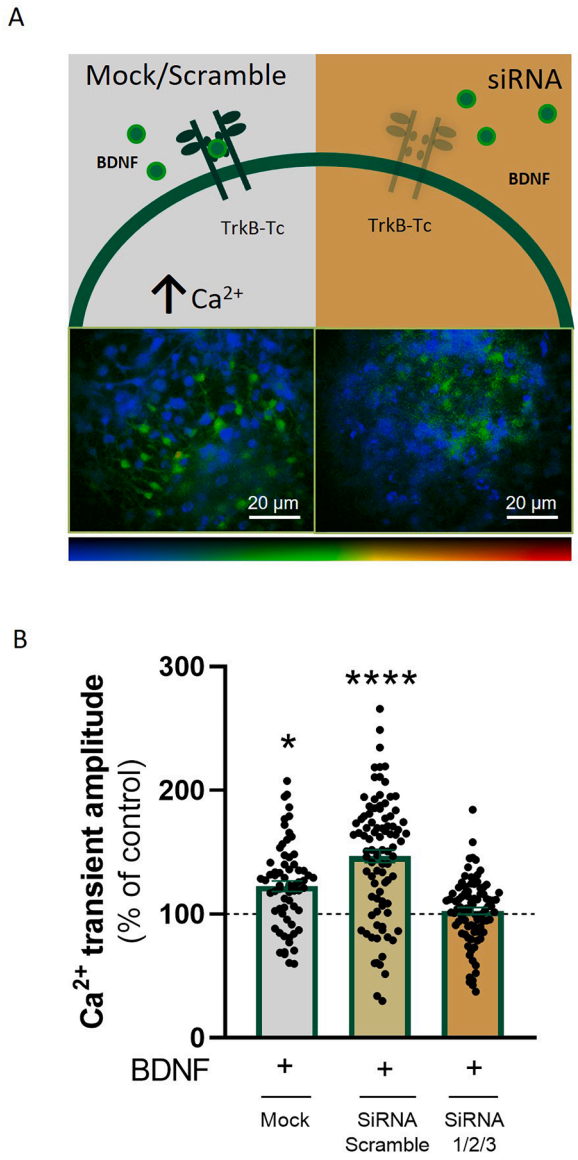

Fig. 4. BDNF effect upon Ca^{2+} transient amplitude in astrocytes transfected with TrkB-T siRNAs. A) Representative scheme of siRNA-mediated effect upon TrkB-Tc signaling in cultures astrocytes (upper panels) and Ca^{2+} images obtained from astrocytes treated with BDNF (20 ng/mL) for 48 h after transfection with the scrambled/mock siRNA or the SiRNAs (lower panel). B) Ca^{2+} transient amplitude in astrocytes 72 h after transfection with the cocktail of the three siRNAs (RNAi 1/2/3), the negative control with scrambled siRNA, and the siRNA mock control, in the presence and absence of BDNF (20 ng/mL). All values are represented as mean ± SEM of n = 3 independent cultures (*$p < 0.05$; ****$p < 0.0001$; significant differences assessed by one-way ANOVA followed by Tukey correction).

[50], Ca^{2+}-permeant ligand-gated channels [4], mGlu5 receptors [51], and P2Y1 receptors [52] in astrocytes. The altered levels of these proteins in astrocytes correlate with changes in astrocytic $[Ca^{2+}]_i$ levels [4,51,52]. These alterations likely underlie the alterations in astrocytic-neuronal communication detected in AD models. In fact, Aβ facilitates Ca^{2+}-dependent astrocytic release of glutamate, which in turn activates extrasynaptic NMDA receptors in neurons, contributing to synaptic loss [4]. In the present work we observed that Aβ increases the amplitude of Ca^{2+} transients elicited by mGluR5 activation, which is in line with current literature [12,14,53,54]. Moreover, a significantly reduced rise time of these responses was observed, indicating a faster onset of intracellular Ca^{2+} elevation. A similar increase of astrocytic Ca^{2+} responses following Aβ exposure have been previously reported and interpreted as enhanced astrocytic Ca^{2+} reactivity rather than cell toxicity [16]. Notably, the decay phase of the Ca^{2+} transients remained unchanged, suggesting that Ca^{2+} clearance mechanisms, including reuptake into intracellular stores or extrusion across the plasma membrane, are not significantly affected under our experimental conditions. A potential limitation related to Ca^{2+} indicator saturation was considered; however, the preserved kinetics of the Ca^{2+} transients and the use of ratiometric Fura-2 imaging support the robustness of our measurements under the experimental conditions used. The selective acceleration of the rising phase is consistent with enhanced efficiency of Ca^{2+} mobilization downstream of mGluR5 activation, likely reflecting increased receptor availability and/or augmented IP_3-dependent Ca^{2+} release from the endoplasmic reticulum [51]. This interpretation aligns with our observation of increased mGluR5 expression following Aβ exposure and with previous reports describing mGluR5 upregulation [51] and astrocytic Ca^{2+} hyperreactivity in Alzheimer's disease models. Importantly, the fact that these kinetic alterations occur in the absence of detectable astrocyte death suggests that Aβ-induced changes in Ca^{2+} signaling represent an early functional dysregulation rather than a consequence of overt toxicity. Such accelerated and amplified Ca^{2+} responses may contribute to aberrant astrocyte–neuron communication and synaptic dysfunction in the early stages of Alzheimer's disease.

The impairment of mGluR5-dependent Ca^{2+} signaling in astrocytes has important functional implications for synaptic transmission and synaptic plasticity [55], being astrocytic Ca^{2+} elevations closely linked to the release of gliotransmitters such as glutamate and D-serine [56], which critically modulate these processes. In the context of Alzheimer's disease, excessive or dysregulated astrocytic Ca^{2+} signaling has been shown to promote aberrant glutamate release, leading to activation of extrasynaptic NMDA receptors and contributing to synaptic dysfunction and loss [4]. Thus, the accelerated and amplified Ca^{2+} responses observed here following Aβ exposure may represent a mechanism by which astrocytes actively participate in early synaptic pathology.

Importantly, our data indicate that BDNF prevents the Aβ-induced upregulation of mGluR5 and the consequent exacerbation of astrocytic Ca^{2+} signaling. This effect suggests a protective role for BDNF in maintaining astrocytic Ca^{2+} homeostasis and limiting maladaptive astrocyte–neuron signaling. By preventing excessive mGluR5-driven Ca^{2+} responses, BDNF may indirectly preserve synaptic integrity and counteract early synaptic dysfunction associated with Aβ pathology. These findings support the concept that BDNF signaling in astrocytes, via TrkB-Tc receptors, is not detrimental but instead contributes to the stabilization of astrocytic function under pathological conditions.

It is worthwhile to mention that, in the present study, we also observed an increase in basal Ca^{2+} levels in astrocytes exposed to $Aβ_{25–35}$ for 48 h and 72 h. This effect has previously been described since astrocytic basal Ca^{2+} levels are abnormal in astrocytes exposed to Aβ oligomers, as well as in several models of AD, such as animals that undergo an intracerebroventricular injection of Aβ oligomers and the triple-transgenic mouse model of AD [14,53,54]. This astrocytic basal Ca^{2+} increase might be attributed to the pore-forming activity mediated by Aβ, known to form Ca^{2+} permeable channels [57], which promotes intracellular Ca^{2+} increases [58]. Moreover, in AD mice models, Aβ plaques trigger connexin 43 (Cx43) hemichannel (HCs) activation that allows Ca^{2+} influx, contributing to a maintenance of high intracellular Ca^{2+} concentration [59]. Moreover, this elevation may result from alterations in intracellular Ca^{2+} stores, including increased endoplasmic reticulum Ca^{2+} leak associated with ER stress [60], to which contributes IP3R and ryanodine receptors' (RyRs) expression and function, dysfunction of the sarco-endoplasmic reticulum Ca^{2+} ATPase (SERCA) activity and upregulation of its truncated isoform (S1T), as well as presenilin (PS1, PS2)-mediated ER Ca^{2+} leak/ER Ca^{2+} release potentiation [60].

Although different studies have pointed to the dysregulation of Ca^{2+} signaling induced by Aβ as the first step for astrocytic degeneration

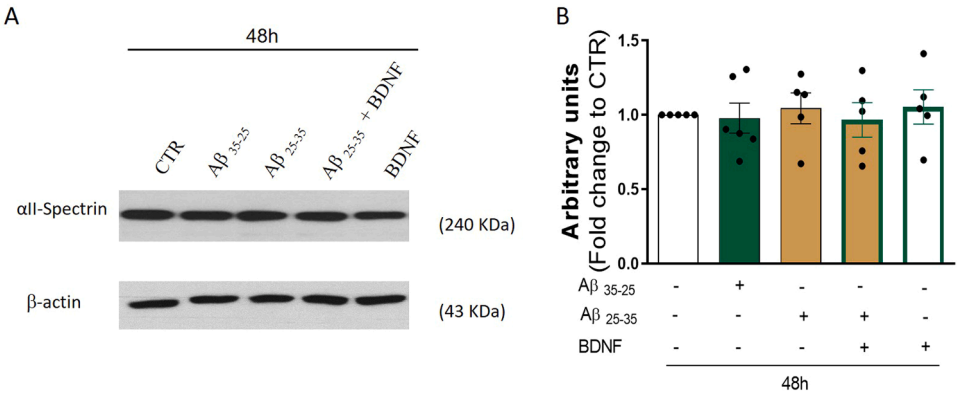

Fig. 5. Effect of Aβ and BDNF on αII-spectrin levels in astrocytes. A) Representative Image of a western blot for the detection of αII-spectrin levels in astrocytes incubated at DIC 10 with $A\beta_{35-25}$ (10 μM), $A\beta_{25-35}$ (10 μM), $A\beta_{25-35}$ (10 μM) + BDNF (20 ng/mL), and BDNF (20 ng/mL) for 48 h. B) Effects of $A\beta_{25-35}$ (10 μM), $A\beta_{25-35}$ (10 μM) + BDNF (20 ng/mL) and BDNF (20 ng/mL) at 48 h upon αII-spectrin levels in astrocytes. Mean ± SEM of n = 5 independent cultures (significant differences assessed by one-way ANOVA followed by Tukey correction).

[61–63], our data do not show apoptotic nor necrotic fingerprints, i.e., cleavage of αII-spectrin and detection of fragment products mediated by caspases and calpains activation respectively. Thus, these results suggest that Aβ treatment for 48 h does not induce cellular death or astrogliosis accordingly to what have been described regardless of the actions of caspases as positive modulators of astrogliosis [64].

Aβ-mediated neurotoxic mechanisms are not fully known, but the existing information suggests that oxidative stress, perturbation of Ca^{2+} homeostasis, mitochondrial dysfunction, synaptic loss, and caspases and calpains activation are strongly involved [65–68]. Calpains are Ca^{2+}-dependent proteases that play a physiologic role by cleaving several substrates. Abnormal activation of calpains and down-regulation of their endogenous inhibitor (calpastatin) have been associated with AD [69–71]. Moreover, calpain overactivation contributes to tau hyperphosphorylation, a hallmark of AD, through the activation of cyclin-dependent kinase 5 (CDK5), followed by the cleavage of its regulatory protein p35 [72–74]. In addition, calpains also contribute to the formation and accumulation of Aβ peptides, and their inhibition prevents neurodegeneration and restores normal synaptic function and spatial memory in AD animal models [75–77]. In our experimental conditions, the absence of calpain and caspase activation in astrocytes treated with Aβ might reinforce that Ca^{2+} signalling dysregulation is an early feature of Aβ-mediated toxicity in astrocytes.

Brain-derived neurotrophic factor (BDNF) is a neurotrophin that promotes neuronal survival, differentiation, and synaptic plasticity through activation of its full-length receptor, TrkB-FL, expressed in neurons. On the contrary, in astrocytes, BDNF exerts its actions mainly through the activation of the truncated isoform of TrkB receptors (TrkB-Tc) [19,20,78]. In addition, $P75^{NRT}$ receptors expressed in neurons and astrocytes can also be activated by this neurotrophin. Alterations in BDNF receptor expression levels have been described in several neurodegenerative disorders. Particularly, hippocampal and cortical *post-mortem* samples from AD patients revealed decreased levels of TrkB-FL and increased levels of TrkB-Tc [23,24,28,79,80. These changes are detected in neurons [29] and justify the BDNF loss of function in synaptic plasticity [29,30], neurotransmitter release [29], and in the modulation of the number of synaptic dentritic spines [30]However, it is worthwhile to notice that, according to our findings, the levels of the astrocytic BDNF TrkB-Tc receptor, were not altered by the exposure to Aβ for up to 48 h.

Rose et al. [19] was the paper that showed that BDNF induces astrocytic $[Ca^{2+}]_i$ release, an effect attributed to TrkB-Tc receptors. The activation of TrkB-Tc receptor by BDNF causes activation of a G protein that stimulates PLC, production of $InsP_3$, and Ca^{2+} release from internal stores (ER) [19]. In our work, we evaluated Ca^{2+} signaling evoked by mGluR5 activation in astrocytes pre-exposed to BDNF and we clearly detected a facilitation of astrocytic $[Ca^{2+}]_i$ transient amplitude, which is mediated by TrkB-Tc receptors. Thus, not only can BDNF trigger astrocytic calcium signalling by itself [19], but it can also facilitate responses triggered by other receptors, such as mGluR5-mediated responses.

Given the similarity of data in the astrocytes exposed to Aβ and to BDNF, we investigated whether BDNF effects on Ca^{2+}signaling could be mediated by an increase in mGluR5 levels. The analysis of mGluR5 levels by western blot led us to conclude that BDNF does not affect mGluR5 levels. Thus, BDNF-induced Ca^{2+} transients are not mediated by an increase of mGluR5 levels and, importantly, BDNF prevents the increase on mGluR5 levels induced by Aβ. Although BDNF does not induce alterations in TrkB-Tc receptor levels, its action upon Ca^{2+}signaling is mediated by TrkB-Tc activation as proven by the absence of effect of BDNF in astrocytes where TrkB-Tc had been downregulated by exposure to siRNA.

We observed a similar effect of BDNF and Aβ on astrocytic Ca^{2+} signaling when added alone to the astrocytes, but when present together, the increase of mGluR5 levels induced by Aβ, as well as the increase of Ca^{2+} transient amplitude was abolished. Having in mind the well-known toxic action of Aβ, one could speculate on the beneficial role of BDNF in astrocytes in AD. Taken together, our data point towards that BDNF, by preventing the increase of mGluR5 levels induced by Aβ, avoids an additive effect on the increase of Ca^{2+} transient amplitude when astrocytes are exposed to both drugs demonstrating that the increase on BDNF levels is not counterproductive in astrocytes.

CRediT authorship contribution statement

Pedro Avelar: Writing – original draft, Methodology, Investigation, Formal analysis, Conceptualization. **Tatiana P. Morais:** Writing – original draft, Methodology, Investigation, Formal analysis, Conceptualization. **Haissa de Castro-Abrantes:** Writing – original draft, Methodology, Investigation, Formal analysis, Conceptualization. **Adam Armada-Moreira:** Writing – review & editing, Writing – original draft, Methodology. **Joana Gonçalves-Ribeiro:** Formal analysis, Methodology. **Cláudia A. Valente:** Writing – review & editing, Methodology. **Ana Maria Sebastião:** Writing – review & editing, Conceptualization. **Maria José Diógenes:** Writing – review & editing, Writing – original draft, Supervision, Investigation, Funding acquisition, Conceptualization. **Sandra H. Vaz:** Writing – review & editing, Writing – original draft, Validation, Software, Investigation, Funding acquisition, Conceptualization.

Declaration of competing interest

The authors declare that they have no known competing financial

interests or personal relationships that could have appeared to influence the work reported in this paper.

Acknowledgments

We thank Regeneron Pharmaceuticals for the gift of brain-derived neurotrophic factor.

This work was supported by project funding from Fundação para a Ciência e para a Tecnologia (FCT) (PTDC/BTM-SAL/32147/2017, PTDC/MED-FAR/30933/2017). This project has received funding from H2020-WIDESPREAD-05–2017-Twinning (EpiEpinet) under grant agreement No 952455. AAM (PD/BD/114278/2016) was supported by a PhD fellowships from FCT.

Supplementary materials

Supplementary material associated with this article can be found, in the online version, at doi:10.1016/j.ceca.2026.103119.

Data availability

Data will be made available on request.

References

[1] F.M. LaFerla, K.N. Green, S. Oddo, Intracellular amyloid-β in Alzheimer's disease, Nat. Rev. Neurosci. 8 (2007) 499–509, https://doi.org/10.1038/nrn2168.
[2] A. Roda, G. Serra-Mir, L. Montoliu-Gaya, L. Tiessler, S. Villegas, Amyloid-beta peptide and tau protein crosstalk in Alzheimer's disease, Neural Regen. Res. 17 (2022) 1666, https://doi.org/10.4103/1673-5374.332127.
[3] A. Armada-Moreira, J.I. Gomes, C.C. Pina, O.K. Savchak, J. Gonçalves-Ribeiro, N. Rei, et al., Going the extra (Synaptic) mile: excitotoxicity as the road toward neurodegenerative diseases, Front. Cell Neurosci. 14 (2020), https://doi.org/10.3389/fncel.2020.00090.
[4] M. Talantova, S. Sanz-Blasco, X. Zhang, P. Xia, M.W. Akhtar, S.I. Okamoto, et al., Aβ induces astrocytic glutamate release, extrasynaptic NMDA receptor activation, and synaptic loss, Proc. Natl. Acad. Sci. U S. A (2013) 110, https://doi.org/10.1073/pnas.1306832110.
[5] C. Agulhon, J. Petravicz, A.A.B. Mcmullen, E.J. Sweger, S.K. Minton, S.R. Taves, et al., What is the role of astrocyte calcium in neurophysiology? Neuron 59 (2008) 932–946, https://doi.org/10.1016/j.neuron.2008.09.004.
[6] A. Araque, M. Navarrete, Glial cells in neuronal network function, Trans. R. Soc. B 365 (2010) 2375–2381, https://doi.org/10.1098/rstb.2009.0313.
[7] J. Gonçalves-Ribeiro, S.H. Vaz, The IP3R2 knockout mice in behavior: a blessing or a curse? J. Neurochem. 169 (2025) https://doi.org/10.1111/jnc.70062.
[8] M. Nedergaard, B. Ransom, S. Goldman, New roles for astrocytes: redefining the functional architecture of the brain, Trends. Neurosci. 26 (2003) 523–530, https://doi.org/10.1016/j.tins.2003.08.008.
[9] G. Perea, M. Navarrete, A. Araque, Tripartite synapses: astrocytes process and control synaptic information, Trends. Neurosci. 32 (2009) 421–431, https://doi.org/10.1016/j.tins.2009.05.001.
[10] R.E. González-Reyes, M.O. Nava-Mesa, K. Vargas-Sánchez, D. Ariza-Salamanca, L. Mora-Muñoz, Involvement of astrocytes in Alzheimer's disease from a neuroinflammatory and oxidative stress perspective, Front. Mol. Neurosci. 10 (2017), https://doi.org/10.3389/fnmol.2017.00427.
[11] M. Ianni, M. Corraliza-Gomez, T. Costa-Coelho, M. Ferreira-Manso, S. Inteiro-Oliveira, N. Alemãn-Serrano, et al., Spatiotemporal dysregulation of neuron–glia related genes and pro-/anti-inflammatory miRNAs in the 5xFAD mouse model of Alzheimer's disease, Int. J. Mol. Sci. 25 (2024), https://doi.org/10.3390/ijms25179475.
[12] L. Lee, P. Kosuri, O. Arancio, Picomolar amyloid-β peptides enhance spontaneous astrocyte calcium transients, J. Alzheimer's Dis. 38 (2014) 49–62, https://doi.org/10.3233/JAD-130740.
[13] A.Y. Abramov, L. Canevari, M.R. Duchen, Changes in intracellular calcium and glutathione in astrocytes as the primary mechanism of amyloid neurotoxicity, J. Neurosci. 23 (2003) 5088–5095.
[14] L. D, I. A, R. V, G. A.A, C. P.L, A. E, et al., Amyloid beta deregulates astroglial mGluR5-mediated calcium signaling via calcineurin and Nf-kB, Glia 61 (2013) 1134–1145.
[15] A. Grolla, G. Fakhfouri, G. Balzaretti, E. Marcello, F. Gardoni, P.L. Canonico, et al., Aβ leads to Ca^{2+} signaling alterations and transcriptional changes in glial cells, Neurobiol. Aging 34 (2013) 511–522, https://doi.org/10.1016/j.neurobiolaging.2012.05.005.
[16] V. Ronco, A.A. Grolla, T.N. Glasnov, P.L. Canonico, A. Verkhratsky, A. A. Genazzani, et al., Differential deregulation of astrocytic calcium signalling by amyloid-β, TNFα, IL-1β and LPS, Cell Calc. 55 (2014) 219–229, https://doi.org/10.1016/j.ceca.2014.02.016.
[17] T. Takano, X. Han, R. Deane, B. Zlokovic, M. Nedergaard, Two-photon imaging of astrocytic Ca2+ signaling and the microvasculature in experimental mice models of Alzheimer's disease, Ann. N Acad. Sci. 1097 (2007) 40–50, https://doi.org/10.1196/annals.1379.004.
[18] A. Grolla, G. Fakhfouri, G. Balzaretti, E. Marcello, F. Gardoni, P.L. Canonico, et al., Aβ leads to Ca^{2+} signaling alterations and transcriptional changes in glial cells, Neurobiol. Aging 34 (2013) 511–522, https://doi.org/10.1016/j.neurobiolaging.2012.05.005.
[19] C.R. Rose, R. Blum, B. Pichler, A. Lepier, K.W. Kafitz, A. Konnerth, Truncated TrkB-T1 mediates neurotrophin-evoked calcium signalling in glia cells, Nature 426 (2003) 74–78, https://doi.org/10.1038/nature01983.
[20] S.H. Vaz, T.N. Jorgensen, S. Cristovao-Ferreira, S. Duflot, J.A Ribeiro, U. Gether, et al., Brain-derived neurotrophic factor (BDNF) enhances GABA transport by modulating the trafficking of GABA transporter-1 (GAT-1) from the plasma membrane of rat cortical astrocytes, J. Biol. Chem. 286 (2011) 40464–40476, https://doi.org/10.1074/jbc.M111.232009.
[21] S.H. Vaz, S.R. Lérias, S. Parreira, M.J. Diógenes, A.M. Sebastião, Adenosine A2A receptor activation is determinant for BDNF actions upon GABA and glutamate release from rat hippocampal synaptosomes, Purinergic. Signal. (2015), https://doi.org/10.1007/s11302-015-9476-1.
[22] B. Chakravarthy, C. Gaudet, M. Ménard, T. Atkinson, L. Brown, F.M. Laferla, et al., Amyloid-β peptides stimulate the expression of the p75NTR neurotrophin receptor in SHSY5Y human neuroblastoma cells and AD transgenic mice, J. Alzheimer's Dis. 19 (2010) 915–925, https://doi.org/10.3233/JAD-2010-1288.
[23] B. Connor, D. Young, Q. Yan, R.L.M. Faull, B. Synek, M. Dragunow, Brain-derived neurotrophic factor is reduced in Alzheimer's disease, Mol. Brain Res. 49 (1997) 71–81, https://doi.org/10.1016/S0169-328X(97)00125-3.
[24] I. Ferrer, C. Marín, M.J. Rey, T. Ribalta, E. Goutan, R. Blanco, et al., BDNF and full-length and truncated TrkB expression in Alzheimer disease. Implications in therapeutic strategies, J. Neuropathol. Exp. Neurol. 58 (1999) 729–739, https://doi.org/10.1097/00005072-199907000-00007.
[25] J. Fonseca-Gomes, T. Costa-Coelho, M. Ferreira-Manso, S. Inteiro-Oliveira, S. H. Vaz, N. Alemãn-Serrano, et al., A small TAT-TrkB peptide prevents BDNF receptor cleavage and restores synaptic physiology in Alzheimer's disease, Mol. Ther. (2024), https://doi.org/10.1016/j.ymthe.2024.08.022.
[26] S. Kemppainen, T. Rantamäki, A. Jerónimo-Santos, G. Lavasseur, H. Autio, N. Karpova, et al., Impaired TrkB receptor signaling contributes to memory impairment in APP/PS1 mice, Neurobiol. Aging 33 (2012) 1122.e23, https://doi.org/10.1016/j.neurobiolaging.2011.11.006. -1122.e39.
[27] C. Miranda-Lourenço, L. Ribeiro-Rodrigues, J. Fonseca-Gomes, S.R. Tanqueiro, R. F. Belo, C.B. Ferreira, et al., Challenges of BDNF-based therapies: from common to rare diseases, Pharmacol. Res. 162 (2020), https://doi.org/10.1016/j.phrs.2020.105281.
[28] H.S. Phillips, J.M. Hains, M. Armanini, G.R. Laramee, S.A. Johnson, J.W. Winslow, BDNF mRNA is decreased in the hippocampus of individuals with Alzheimer's disease, Neuron 7 (1991) 695–702, https://doi.org/10.1016/0896-6273(91)90273-3.
[29] A. Jerónimo-Santos, S.H. Vaz, S. Parreira, S. Rapaz-Lérias, A.P. Caetano, V. B. Scherrer, et al., Dysregulation of TrkB Receptors and BDNF function by amyloid-β peptide is mediated by calpain, Cereb. Cortex. 25 (2015) 3107–3121, https://doi.org/10.1093/cercor/bhu105.
[30] S.R. Tanqueiro, R.M. Ramalho, T.M. Rodrigues, L.V. Lopes, A.M. Sebastião, M. J. Diógenes, Inhibition of NMDA receptors prevents the loss of BDNF function induced by amyloid β, Front. Pharmacol. 9 (2018) https://doi.org/10.3389/fphar.2018.00237.
[31] K. Ohira, H. Kumanogoh, Y. Sahara, K.J. Homma, H. Hirai, S. Nakamura, et al., A truncated tropomyosin-related kinase B receptor, T1, regulates glial cell morphology via Rho GDP dissociation inhibitor 1, J. Neurosci. 25 (2005) 1343–1353, https://doi.org/10.1523/JNEUROSCI.4436-04.2005.
[32] T.P. Morais, D. Coelho, S.H. Vaz, A.M. Sebastião, C.A. Valente, Glycine receptor activation impairs ATP-induced calcium transients in cultured cortical astrocytes, Front. Mol. Neurosci. 10 (2018), https://doi.org/10.3389/fnmol.2017.00444.
[33] C. Abild Meyer, P. De Dios Andres, E. Brodszkij, I.N. Westensee, J. Lyons, S.H. Vaz, B. Städler, Astrocytes in Paper Chips and Their Interaction with Hybrid Vesicles, Adv. Biol. (Weinh). 7 (1) (2023) e2200209, https://doi.org/10.1002/adbi.202200209.
[34] K.D. McCarthy, J. De Vellis, Preparation of separate astroglial and oligodendroglial cell cultures from rat cerebral tissue, J. Cell Biol. 85 (1980) 890–902, https://doi.org/10.1083/jcb.85.3.890.
[35] P.F. Jacob, S.H. Vaz, J.A. Ribeiro, A.M. Sebastião, P2Y1 receptor inhibits GABA transport through a calcium signalling-dependent mechanism in rat cortical astrocytes, Glia 62 (2014) 1211–1226, https://doi.org/10.1002/glia.22673.
[36] R. Barhoumi, Y. Qian, R.C. Burghardt, E. Tiffany-Castiglioni, Image analysis of Ca2 + signals as a basis for neurotoxicity assays: promises and challenges, Neurotoxicol. Teratol. 32 (2010) 16–24, https://doi.org/10.1016/j.ntt.2009.06.002.
[37] a H.J. Knot, I. Laher, E. Sobie, S. Guatimosim, L. Gomez-Viquez, H. Hartmann, et al., Twenty years of calcium imaging: cell physiology to dye for, Mol. Interv. 5 (2005) 112–127, https://doi.org/10.1124/mi.5.2.8.
[38] R.F. Lopes, J. Gonçalves-Ribeiro, A.M. Sebastião, et al., SIGAA: signaling automated analysis: a new tool for Ca2+ signaling quantification using ratiometric Ca2+ dyes, SIViP 18 (2024) 1273–1284, https://doi.org/10.1007/s11760-023-02821-7.
[39] C.A. Schneider, W.S. Rasband, K.W. Eliceiri, NIH Image to ImageJ: 25 years of image analysis, Nat. Methods 9 (2012) 671–675.

[40] R.I. Aroeira, A.M. Sebastião, C.A. Valente, BDNF, via truncated TrkB receptor, modulates GlyT1 and GlyT2 in astrocytes, Glia 63 (2015) 2181–2197, https://doi.org/10.1002/glia.22884.
[41] G. Grynkiewicz, M. Poenie, R.Y. Tsien, A new generation of Ca2+ indicators with greatly improved fluorescence properties, J. Biol. Chem. 260 (6) (1985) 3440–3450. Mar 25PMID: 3838314.
[42] T. Nakamura, K. Nakamura, N. Lasser-Ross, J.G. Barbara, V.M. Sandler, W.N. Ross, Inositol 1,4,5-trisphosphate (IP3)-mediated Ca2+ release evoked by metabotropic agonists and backpropagating action potentials in hippocampal CA1 pyramidal neurons, J. Neurosci. 20 (22) (2000) 8365–8376, https://doi.org/10.1523/JNEUROSCI.20-22-08365.2000. Nov 15PMID: 11069943; PMCID: PMC6773168.
[43] R. Rizzuto, D. De Stefani, A. Raffaello, C. Mammucari, Mitochondria as sensors and regulators of calcium signalling, Nat. Rev. Mol. Cell Biol. 13 (9) (2012) 566–578, https://doi.org/10.1038/nrm3412. SepEpub 2012 Aug 1. PMID: 22850819.
[44] D.F. Condorelli, P. Dell'Albani, G. Mudò, T. Timmusk, N. Belluardo, P.D. Albani, et al., Expression of neurotrophins and their receptors in primary astroglial cultures: induction by cyclic AMP-elevating agents, J. Neurochem. 63 (1994) 509–516.
[45] J.D. Roback, N.H. Marsh, M. Downen, H.C. Palfrey, B.H. Wainer, BDNF-activated signal transduction in rat cortical glial cells, Eur. J. Neurosci. 7 (1995) 849–862, https://doi.org/10.1111/j.1460-9568.1995.tb01072.x.
[46] J.S.J.S. Rudge, Y. Li, E.M.E.M. Pasnikowski, K. Mattsson, L. Pan, G.D.G. D. Yancopoulos, et al., Neurotrophic factor receptors and their signal transduction capabilities in rat astrocytes, Eur. J. Neurosci. 6 (1994) 693–705.
[47] Y. Cai, H.X. Zhu, J.M. Li, X.G. Luo, P.R. Patrylo, G.M. Rose, et al., Age-related intraneuronal elevation of αII-spectrin breakdown product SBDP120 in rodent forebrain accelerates in 3×Tg-AD mice, PLoS. One 7 (2012) 1–12, https://doi.org/10.1371/journal.pone.0037599.
[48] T. Kubo, S. Nishimura, Y. Kumagae, I. Kaneko, In vivo conversion of racemized βamyloid ([D-Ser26]Aβ1-40) to truncated and toxic fragments ([D-Ser26]Aβ25-35/40) and fragment presence in the brains of Alzheimer's patients, J. Neurosci. Res. 70 (2002) 474–483, https://doi.org/10.1002/jnr.10391.
[49] C.J. Pike, A.J. Walencewicz-Wasserman, J. Kosmoski, D.H. Cribbs, C.G. Glabe, C. W. Cotman, Structure-activity analyses of β-amyloid peptides: contributions of the β25-35 region to aggregation and neurotoxicity, J. Neurochem. 64 (2002) 253–265, https://doi.org/10.1046/j.1471-4159.1995.64010253.x.
[50] T. Teaktong, A. Graham, J. Court, R. Perry, E. Jaros, M. Johnson, et al., Alzheimer's disease is associated with a selective increase in α7 nicotinic acetylcholine receptor immunoreactivity in astrocytes, Glia 41 (2003) 207–211, https://doi.org/10.1002/glia.10132.
[51] D. Lim, A. Iyer, V. Ronco, A.A. Grolla, P.L. Canonico, E. Aronica, et al., Amyloid beta deregulates astroglial mGluR5-mediated calcium signaling via calcineurin and Nf-kB, Glia 61 (2013) 1134–1145, https://doi.org/10.1002/glia.22502.
[52] A. Delekate, M. Füchtemeier, T. Schumacher, C. Ulbrich, M. Foddis, G.C. Petzold, Metabotropic P2Y1 receptor signalling mediates astrocytic hyperactivity in vivo in an Alzheimer's disease mouse model, Nat. Commun. 5 (2014), https://doi.org/10.1038/ncomms6422.
[53] E. Alberdi, A. Wyssenbach, M. Alberdi, M.V. Sánchez-Gómez, F. Cavaliere, J. J. Rodríguez, et al., Ca2+-dependent endoplasmic reticulum stress correlates with astrogliosis in oligomeric amyloid β-treated astrocytes and in a model of Alzheimer's disease, Ag. Cell 12 (2013) 292–302, https://doi.org/10.1111/acel.12054.
[54] N.J. Haughey, M.P. Mattson, Alzheimer's amyloid β-peptide enhances ATP/Gap junction-mediated calcium-wave propagation in astrocytes, Neuromolecular. Med. 3 (2003) 173–180, https://doi.org/10.1385/NMM:3:3:173.
[55] J.D. Dias, J.F. Viana, L.S. Alves, A. Veiga, B. Matos, J.L. Machado, J.F. Oliveira, AstroWars: the return of the astrocytic metabotropic glutamate receptor 5, J. Physiol. (2025), https://doi.org/10.1113/JP288403. Apr 4Epub ahead of print. PMID: 40184039.
[56] D.S. Abreu, J.I. Gomes, F.F. Ribeiro, M.J. Diógenes, A.M. Sebastião, S.H. Vaz, Astrocytes control hippocampal synaptic plasticity through the vesicular-dependent release of D-serine, Front. Cell Neurosci. 17 (2023) 1282841, https://doi.org/10.3389/fncel.2023.1282841. Dec 7PMID: 38145284; PMCID: PMC10740624.
[57] N. Arispe, E. Rojas, H.B. Pollard, Alzheimer disease amyloid beta protein forms calcium channels in bilayer membranes: blockade by tromethamine and aluminum, Proc. Natl. Acad. Sci. U S. A 90 (1993) 567–571, https://doi.org/10.1073/pnas.90.2.567.
[58] A.Y. Abramov, L. Canevari, M.R. Duchen, Changes in intracellular calcium and glutathione in astrocytes as the primary mechanism of amyloid neurotoxicity, J. Neurosci. 23 (2003) 5088–5095.
[59] C. Yi, A. Koulakoff, C. Giaume, New insights on astroglial connexins as a therapeutic target for Alzheimer's disease, J. Cell Signal. (2017) 02, https://doi.org/10.4172/2576-1471.1000162.
[60] M. Chami, F. Checler, Alterations of the endoplasmic reticulum (ER) calcium signaling molecular components in Alzheimer's disease, Cells 9 (12) (2020) 2577, https://doi.org/10.3390/cells9122577. Dec 1PMID: 33271984; PMCID: PMC7760721.
[61] J.J. Rodríguez, M. Olabarria, A. Chvatal, A. Verkhratsky, Astroglia in dementia and Alzheimer's disease, Cell Death. Differ. 16 (2009) 378–385, https://doi.org/10.1038/cdd.2008.172.
[62] A. Verkhratsky, M. Olabarria, H.N. Noristani, C.-Y. Yeh, J.J. Rodriguez, Astrocytes in Alzheimer's disease, Neurotherapeutics 7 (2010) 399–412.
[63] A.J. Vincent, R. Gasperini, L. Foa, D.H. Small, Astrocytes in Alzheimer's disease: emerging roles in calcium dysregulation and synaptic plasticity, J. Alzheimers. Dis. 22 (2010) 699–714, https://doi.org/10.3233/JAD-2010-101089.
[64] R. Aras, A.M. Barron, C.J. Pike, Caspase activation contributes to astrogliosis, Brain Res. 1450 (2012) 102–115, https://doi.org/10.1016/j.brainres.2012.02.056.
[65] C. Hölscher, Possible causes of Alzheimer's disease: amyloid fragments, free radicals, and calcium homeostasis, Neurobiol. Dis. 5 (3) (1998) 129-41, https://doi.org/10.1006/nbdi.1998.0193.
[66] C. Hölscher, Development of beta-amyloid-induced neurodegeneration in Alzheimer's disease and novel neuroprotective strategies, Rev. Neurosci. 16 (3) (2005) 181–212, https://doi.org/10.1515/revneuro.2005.16.3.181.
[67] D.J. Selkoe, Alzheimer's disease is a synaptic failure, Science 298 (5594) (2002) 789-91, https://doi.org/10.1126/science.1074069.
[68] Z. Wei, M.S. Song, D. MacTavish, J.H. Jhamandas, S. Kar, Role of calpain and caspase in beta-amyloid-induced cell death in rat primary septal cultured neurons, Neuropharmacology 54 (4) (2008) 721-33, https://doi.org/10.1016/j.neuropharm.2007.12.006.
[69] K. Saito, J.S. Elce, J.E. Hamos, R.A. Nixon, Widespread activation of calcium-activated neutral proteinase (calpain) in the brain in Alzheimer disease: a potential molecular basis for neuronal degeneration, Proc. Natl. Acad. Sci. USA 90 (7) (1993) 2628-32, https://doi.org/10.1073/pnas.90.7.2628.
[70] F. Grynspan, W.R. Griffin, A. Cataldo, S. Katayama, R.A. Nixon, Active site-directed antibodies identify calpain II as an early-appearing and pervasive component of neurofibrillary pathology in Alzheimer's disease, Brain Res 763 (2) (1997) 145-58, https://doi.org/10.1016/s0006-8993(97)00384-3.
[71] E. Adamec, P. Mohan, J.P. Vonsattel, R.A. Nixon, Calpain activation in neurodegenerative diseases: confocal immunofluorescence study with antibodies specifically recognizing the active form of calpain 2, Acta Neuropath. 104 (1) (2002) 92–104, https://doi.org/10.1007/s00401-002-0528-6.
[72] M.S. Lee, Y.T. Kwon, M. Li, J. Peng, R.M. Friedlander, L.H. Tsai, Neurotoxicity induces cleavage of p35 to p25 by calpain, Nature 405 (6784) (2000) 360-4, https://doi.org/10.1038/35012636.
[73] W. Noble, V. Olm, K. Takata, E. Casey, O. Mary, J. Meyerson, K. Gaynor, J. LaFrancois, L. Wang, T. Kondo, P. Davies, M. Burns, Veeranna, R. Nixon, D. Dickson, Y. Matsuoka, M. Ahlijanian, L.F. Lau, K. Duff, Cdk5 is a key factor in tau aggregation and tangle formation in vivo, Neuron 38 (4) (2003) 555-65, https://doi.org/10.1016/s0896-6273(03)00259-9.
[74] J.C. Cruz, L.H. Tsai, Cdk5 deregulation in the pathogenesis of Alzheimer's disease, Trends Mol. Med. 10 (9) (2004) 452-8, https://doi.org/10.1016/j.molmed.2004.07.001.
[75] F. Trinchese, M. Fa', S. Liu, H. Zhang, A. Hidalgo, S.D. Schmidt, H. Yamaguchi, N. Yoshii, P.M. Mathews, R.A. Nixon, O. Arancio, Inhibition of calpains improves memory and synaptic transmission in a mouse model of Alzheimer disease, J. Clin. Invest. 118 (8) (2008) 2796-807, https://doi.org/10.1172/JCI34254.
[76] I. Granic, C. Nyakas, P.G. Luiten, U.L. Eisel, L.G. Halmy, G. Gross, H. Schoemaker, A. Möller, V. Nimmrich, Calpain inhibition prevents amyloid-beta-induced neurodegeneration and associated behavioral dysfunction in rats, Neuropharmacology 59 (4–5) (2010) 334-42, https://doi.org/10.1016/j.neuropharm.2010.07.013.
[77] R. Medeiros, M. Kitazawa, M.A. Chabrier, D. Cheng, D. Baglietto-Vargas, A. Kling, A. Moeller, K.N. Green, F.M. LaFerla, Calpain inhibitor A-705253 mitigates Alzheimer's disease-like pathology and cognitive decline in aged 3xTgAD mice, Am. J. Pathol. 181 (2) (2012) 616-25, https://doi.org/10.1016/j.ajpath.2012.04.020.
[78] R.I. Aroeira, A.M. Sebastião, C.A. Valente, BDNF, via truncated TrkB receptor, modulates GlyT1 and GlyT2 in astrocytes, Glia 63 (2015) 2181–2197, https://doi.org/10.1002/glia.22884.
[79] S.J. Allen, G.K. Wilcock, D. Dawbarn, Profound and selective loss of catalytic TrkB immunoreactivity in Alzheimer's disease, Biochem. Biophys. Res. Commun. 264 (3) (1999) 648-51, https://doi.org/10.1006/bbrc.1999.1561.
[80] R.M. Holsinger, J. Schnarr, P. Henry, V.T. Castelo, M. Fahnestock, Quantitation of BDNF mRNA in human parietal cortex by competitive reverse transcription-polymerase chain reaction: decreased levels in Alzheimer's disease, Brain Res. Mol. Brain. Res. 76 (2) (2000) 347-54, https://doi.org/10.1016/s0169-328x(00)00023-1.